KINETIC AND MECHANISTIC ASPECTS OF CO_2 GASIFICATION ON ALKALI TREATED CARBON

C. T. Ratcliffe*

Corporate Research - Science Laboratory
Exxon Research and Engineering
Route 22 East, Annandale, N. J. 08801

Introduction

While catalysis of CO_2 gasification of carbon or coal chars by alkali metals has been the subject of many investigations (1), the state of the catalyst site during gasification and the mechanism involved in the rate limiting step have yet to be resolved. An inherent problem in catalyzed gas-solid reactions at the required high temperatures is the inability to separate the reaction into discrete steps which can be monitored under isothermal reaction conditions. The approach taken in this study has been to decouple the reaction into three steps: catalyst activation, CO_2 chemisorption and reaction/desorption, with only the adsorption step examined under isothermal conditions. The strong chemisorption of CO_2 on thermally activated potassium sites, which showed similarities via our MAS-NMR analysis to the electrostatically held CO_2 on alkali treated Al_2O_3 or SiO_2-Al_2O_3 catalysts as reported by Krupay et al. (2), Sefcik et al. (3,4) and Barrer et al. (5) has allowed the population of active sites to be measured by the quantity of CO_2 that irreversibly chemisorbed at 300°C on the active surface (6). The state of this intermediate is similar to the type suggested much earlier by Long and Sykes (7) and more recently by Mims and Pabst (8), but in disagreement with a mechanism involving K_2CO_3 formation and subsequent reduction to the metal as proposed by McKee (9) and Vera and Bell (10).

The objective of this study has been to examine the thermochemical reaction(s) of each adsorbed CO_2 complex with an atom of carbon on the surface to eventually yield two molecules of CO. Isotope labelled $^{13}CO_2$ has been adsorbed on the active sites so that the reaction chemistry of CO_2 with the carbon lattice could be monitored by Temperature Programmed Desorption (TPD) with the carbon label differentiated by mass spectral examination of the products. While the TPD analysis technique has been primarily employed for examining desorption of single crystal catalyst surfaces (11), the technique can be applied to porous catalyst materials with proper precautions (12). If discrete desorption states can be identified, details of the kinetics of desorption process can be obtained (13). Feats and Keep have examined graphite (thermal or reactor irradiated) after CO_2 or O_2 adsorption by TPD and found discrete states for desorption of CO and CO_2 (14). Linear TPD analysis and a step-TPD technique were studied by Tremblay et al. to determine the energetics of oxygen removel as CO from non-catalyzed carbons. These authors summarized their results with two major points; more than one functional group is present on carbon and the activation energies for these complexes must be a distributed function (15). Frericks has reported TPD spectra for CO_2 and H_2O on potassium doped carbon samples but the spectra were not analyzed for kinetic information (16).

* Present Address: Union Oil Company of California, Science and Technology Division, P. O. Box 76, Brea, California 92621

Discrete desorption states for 13-labelled CO and lattice carbon derived CO have been obtained in this study by TPD at one atmosphere in a flowing inert gas stream. Analysis of the TPD spectra by the methods outlined by Redhead, Cvetanovic and Amenomiya and Taylor and Weinberg are presented (11,13,17).

EXPERIMENTAL

Samples and Reagents

Spherocarb, a low ash form of activated carbon with a surface area of 800 m^2/g, was purchased from Analabs Inc., New Haven, Connecticut. Isotope labelled $^{13}CO_2$ (98% ^{13}C) was purchased from Isotec, Inc., Centerville, Ohio, with the percentage isotope label verified by M.S. analysis. A high purity source of He (99.9999%) was used as a carrier gas in all experiments. The He stream was passed through a heated trap containing Cu turnings for O_2 removal followed by molecular sieve traps to insure H_2O removal. The purity of He was found to be critical in adsorption/desorption runs on carbon and was checked periodically by verifying a constant weight of carbon in the TGA/DSC at elevated temperatures (800°C) while flowing a He stream for 2-3 hour period.

Potassium carbonate was purchased from B&A Chemicals (reagent grade). Aqueous solution of K_2CO_3 were used to impregnate Spherocarb samples with the volume of the aqueous solution equated to the quantity of moisture required to fully wet the surface but not allow excess solution (method of incipient wetness). After impregnation, samples were dried to 60-70°C in a vacuum oven and sealed in glass containers under inert atmosphere.

Isothermal adsorption and temperature programmed desorption runs were performed in a Mettler 2000C TGA/DSC Analyzer. The balance platform, sample crucibles and chamber were constructed of α-alumina with no artifacts in adsorption of desorption noted in blank runs. Analysis of the exit gas was performed with a UTI model 100 mass spectrometer that was interfaced with a Spectra Link unit to a MINC 1123 laboratory computer. Multiple ions could be monitored on a continuous basis during TPD runs. In a typical run, eight amu valves were monitored in a cyclic manner in which data for each mass unit was collected for one second with a total cycle comprising about ten seconds. In this manner, a sufficient number of counts could be obtained for each ion to provide an accurate ratio of partial pressures while the frequency of cycling was fast enough to gain peak temperatures (T_p) for CO and CO_2 fragments at programming rates up to 0.5 K/sec. A small portion (5-10%) of the exit flow from the reaction chamber was differentially pumped through a capillary tube to minimize lag time to the M.S. chamber. The flow pattern, as outlined on Figure #1, was designed to minimize readsorption during TPD experiments (12).

Adsorption of CO_2 was always performed with 90% He dilution. Samples of K_2CO_3-Spherocarb were preconditioned by heating to 850°C in an inert gas flow prior to the adsorption/TPD study. After an isothermal temperature was established, the adsorption was carried out at 60°C followed by a period of approximately one hour to purge the chamber of residual CO_2.

RESULTS AND DISCUSSION

Product Formation and Isotope Distribution

The profile of desorbed products, as shown in Figures 2 and 3, identifies three regions of desorption for CO. Desorption of CO_2 can also be detected in much

lower concentrations with a low temperature peak centered at 170°C and a broad desorption peak at 500°C. The C-13 label on adsorbed CO_2 readily differentiates the source of carbon for both CO and CO_2. Desorption of CO with mass 29 is clearly present in peaks at 200°, 490°, and 685°, while mass 28 (CO from lattice carbon) is only observed in the 750°C peak. Only labelled CO_2 (mass 45) can be seen in the desorption spectra. The lack of coincidence in desorption states for ^{13}CO or ^{12}CO should be noted as it indicates distinct desorption processes. Adsorption of CO_2 at isothermal temperatures from 25-100°C had no effect on the relative ratio of products or the peak maxima. Higher temperature adsorption of CO_2 decreased the contribution of the lower temperature states in the TPD spectrum. Continued evolution of CO above 800°C is also evident in all the spectra. Removal of tightly bound oxygen in chars is known to require very high temperatures (1000°C in vacuum) (18,19) in addition to eventually volatilizing the alkali metal (20). The chemistry in this temperature region was not examined as it is not relevant to the catalytic reaction.

Continued cycling of CO_2 adsorption at 25°C or 100°C followed by TPD programming to 800-850°C demonstrated the reproducible stoichiometry of the Boudouard reaction as monitored during each cycle with the TGA unit:

$$CO_2(44\ \text{amu}) + C(12\ \text{amu}) \rightarrow 2CO\ (56\ \text{amu}).$$

Thus, separation of the adsorption process and the subsequent thermal desorption into separate steps allowed gasification to be performed on a "one turnover" per cycle basis. That is, for each active site that chemisorbed one molecule of CO_2, one atom of lattice carbon was reacted during the TPD process to yield two molecules of CO. The quantity of adsorbed CO_2 could readily be controlled by introducing a limited amount of CO_2 into the gas stream and observing the weight gain with the TGA. Thus the effect of desorption at different loading levels could be quantified with the measured weight of adsorbed CO_2 and desorbed CO as known gravimetric values and the isotope contribution determined from the area under the mass spectral profiles. The TPD profiles in Figures 2-4 correspond to desorption of a full saturation of chemisorbed sites (0.6 sites/mole of K_2CO_3 impregnated). A decline in the total mass of desorbed ^{13}CO as compared to ^{12}CO with lower loadings was observed upon integrating the area under the respective M.S. profiles shown in Figures 2 and 4. A similar decrease in the ratio of $^{13}CO/^{12}CO$ was noted with equal coverages of CO_2 but decreasing ramping rates. Readsorption of ^{13}CO after its release from lower energy binding states appears probable from these results with a visual illustration of the decline in ^{13}CO with lower loading shown in Figure 4.

Adsorption of CO_2 at elevated isothermal temperatures was examined up to 500°C. TPD analysis of the surface after adsorption at elevated temperatures showed a dominance of CO desorption in the anticipated 700°C region, with little contribution from the lower states.

Determination of Rate Parameters via TPD Analysis

Interpretation of TPD spectra allows the activation energy, frequency factor and order of a process to be determined as the shape of the peaks and the position of the peaks maxima bear a fundamental relationship to the desorption process (11-13).

Data obtained from TPD spectra with variable surface coverage was analyzed from the basic equation,

$$\frac{E_d}{RT_p^2} = \frac{V^n}{\beta} \quad C^{n-1} \exp \frac{-E_d}{RT_p} \qquad (1)$$

n = reaction order
C = surface conc.
V = frequency factor
E_d = activation energy
T_p = peak desorp. temp.
β = ramping rate

Rearrangement of this equation reveals the dependence of surface concentration on temperature as a function of reaction order.

$$C^{n-1} = \exp. \frac{E_d}{RT_p} \cdot \frac{E_d \beta}{RT_p^2 V^n} \qquad (2)$$

If little change in the energy or frequency factor is assumed as a function of loading level, the relative shift of T_p as a function of C will allow a determination of the reaction order. The temperature of the desorption peak for lattice derived carbon (^{12}C) remained constant in the region of surface coverages used in this study (40-100%) and thus represented the profile of a first order desorption process. The three desorption peaks for ^{13}CO (derived from $^{13}CO_2$) also showed constant T_p values at surface coverages in the range mentioned above as shown in Figure #3 which is consistent with first order desorption processes.

TPD experiments were also performed at constant surface coverage values of CO_2, as measured with the thermal balance, and at variable heating rates of 0.5 K/sec. to 0.033 K/sec. Surface coverages above 80% were used in all cases. Analysis of the activation energies and preexponential factors could be determined from the log form of equation (1) as mass transfer problems were not anticipated based on the design parameters of Gorte (12) and the effect of readsorption on the preexponential term was small compared to the error in the intercept under the conditions of this study (21). Adsorption of CO on this surface had also been shown by independent studies to be a non-activated process, thus $\Delta H = E_d$.

$$2 \ln T_p - \ln \beta = \frac{E_d}{RT_p} - \ln \frac{V^n R}{E_d} \qquad (3)$$

The values of T_p were obtained from both the mass spectral plot and the DTGA peak from the weight loss profile. Desorption of ^{13}CO in the higher temperature region required dependence on only the M.S. values as the derivative weight loss peak (DTGA) usually appeared as a shoulder on the larger ^{12}CO peak. The series of M.S. spectra generated from the desorption of m/e = 28 at different β values is shown in Figure 5. The values of T_p, which required a temperature correction for heat transport effects, were utilized to calculate parameters for activation energies and factors. The desorption energy for the lower temperature release of ^{13}CO, as shown in Figure 6, gave a value of 45 ± 3 Kcal/mole with a frequency factor of 4×10^{12}. Desorption of ^{12}CO and ^{13}CO at the higher temperature region revealed higher energy values of 73 ± 3 Kcal/mole and 72 ± 5 Kcal/mole, respectively with frequency factors of 10^{15}-10^{16} range for both processes (see Figures 7,8). The temperature dependence

plot for ^{12}CO in Figure 7 displays the experimental values for DTGA and M.S. derived values of T_p while Figure 6 and 8 were taken from mass spectral profiles.

Energetics and Mechanism of CO Formation and Desorption

Exothermic adsorption of CO_2 on discrete alkali containing sites results in the formation of a CO_2 containing complex that appears stable up to 400°C. The chemical shift of 13 labelled carbon (from adsorbed CO_2) by MAS-NMR clearly showed that K_2CO_3 and $KHCO_3$ have not formed, but the surface intermediate appears to be "carbonate" in nature. Temperature programmed desorption up to 400°C in this study revealed no enthalpy changes as noted with the DSC probe, precluding any chemical change involving gain or loss of energy although CO and CO_2 evolution from weakly held sites occurred at 200°C. Thus, the breaking of the CO_2 complex on a potassium salt treated carbon surface to transfer oxygen and the desorption of CO appear to occur as a single endothermic process at 400°C. This transfer of oxygen and desorption of CO most probably is catalyzed by the potassium site. Bonner and Turkevich (22), Lang and Magnier (23) and Tonge (24) have independently studied the transfer of oxygen from CO_2 to different forms of non-catalyzed graphite of carbon. Desorption of CO was found to occur at temperatures as low as 450°C (Tonge) although the rate of exchange of oxygen from CO_2 to carbon was very low (1700 hrs for completion at 500°C) and the surface coverage was minimal (7×10^{-6} C atom sites/C atom). The inability to desorb all the labelled ^{13}CO in this study at the 400°C endothermic transition, either due to readsorption of CO or the presence of more than one type of site, precludes any statement from this study claiming a single event for the first step in the classic mechanism of CO_2 gasification as outlined by Long and Sykes (25), where (0) refers to an adsorbed oxygen on the carbon surface.

$$CO_2 \rightarrow (0) + CO \qquad (a)$$
$$C + (0) \rightarrow CO \qquad (b)$$

The demonstrated ability of K-Spherocarb to chemisorb CO, with eventual desorption of the majority of the oxygen from a higher dissociated state, places more emphasis on the third step in above mechanism of gasification as shown below:

$$CO \underset{j}{\overset{i}{\rightleftharpoons}} (CO). \qquad (c)$$

While readsorption of CO was not found to be significant in the kinetic study with carbon (8,25) it may be important with potassium treated carbon. The desorption energy for the removal of CO at 490°C from K-Spherocarb via TPD analysis in this study (45 $\pm$ 3 Kcal/mole) with a frequency factor of 10^{12} represent a considerably more facile process than the initial transfer process of Long and Sykes (a) for extracted charcoal (Eact = 68, V = 3×10^9) or for the original charcoal (Eact = 58.8 Kcal, V = 6×10^8) (8). Our studies of CO adsorption on K-Spherocarb showed a non-activated process (thus $\Delta H_{desorp.}$ = Eact); the lower activation energy and higher pre-exponential factor therefore represent the catalytic activity of potassium in this first step (a). The low temperature transition for release of oxygen on alkali treated carbon surfaces is consistent with earlier oxygen exchange studies (19-22) in addition to the aforementioned work by Long and Sykes (8,25).

The energetics and isotope distribution of CO adsorption states allows additional insight on the nature of the surface complexes. The release of CO above 600°C involves separate and discrete sites for lattice derived carbon and CO_2

derived carbon as distinguished by the carbon isotope label. The relative increase in the quantity of ^{13}CO desorbed in the 600-700°C region with a decrease in coverage of adsorbed $^{13}CO_2$ is consistent with preferential bonding to this site (either directly or by readsorption) vs the weaker sites desorbing at 490 and 200°C. As the total quantity of desorbed ^{13}CO is similar to desorbed ^{12}CO, and much greater than the predicted quantity of lattice carbon exposed on the higher surface area Spherocarb, the labelled carbon must be either bonded to or in close proximity to an oxygen atom. The similarity of the desorption enthalpy for ^{13}CO and ^{12}CO above 600°C also implies a similar form of bound intermediate, although the desorption profile always revealed ^{13}CO evolution at a lower temperature than ^{12}CO. The high activation energy for the above processes is equal or greater than values reported for CO release by others from non-catalyzed carbon system. The value of 59 Kcal reported by Ergun (26,27) on three different carbons (Ceylon Graphite, activated graphite and activated carbon) and the value of 67 Kcal for graphite reported by Tyso (28) et al. were obtained under controlled differential flow conditions. A recent steady state kinetic investigation by Freund (29) has shown an activation energy of 58 ± 3 Kcal for CO_2 gasification of catalyzed and non-catalyzed carbon samples.

The higher energy values obtained in this TPD investigation as compared to steady state kinetic results is probably not due to CO inhibition problems as they have been accounted for in the above quote studies. The inability to measure accurate reaction bed temperatures during the endothermic gasification presents a more plausible explanation. The temperature values obtained in our TPD study, despite the small sample size and low concentration of adsorbed CO_2, required a correction at higher temperatures due to the endotherm of CO desorption. The actual temperature of our desorption peaks were corrected with factors determined from DSC measurement of the melting of metals (also an endothermic process) at the desorption temperature. Localized cooling of the bed during any steady state kinetic run would also result in artificially high temperatures from a thermocouple value which would lower the value of the calculated activation energy from a reaction rate vs. reciprocal temperature plot.

CONCLUSIONS

Isotope labelled TPD under one atmosphere inert gas flow has provided a method of decoupling alkali catalyzed gasification into steps. Distinct desorption states for CO have been identified which help explain the mechanism of CO_2 interaction with the alkali catalyzed carbon surface. The rate limiting step has been shown to involve removal of lattice carbon as CO. As the activation energy for this step does not appear to be lowered by potassium, alkali serves as a catalyst by increasing the number of active sites in CO_2 gasification of carbon and exchanging oxygen from CO_2 to the carbon surface.

Acknowledgments

The author wishes to thank R. A. Salher for technical assistance in the experimental program.

REFERENCES

1. W-Y. Wen Catal. Rev. Sci. Eng 22 (1) 1-28, (1980); D. W. McKee, Chemistry and Physics of Carbon, 16, Marcel Dekker, New York, 1981; International Symposium on the Fundamentals of Catalyzed Coal Gasification, Fuel, 62 (1983).
2. B. Krupay, Y. Amenomiya, J. Catalysis 67, 362 (1981).
3. M. D. Sefcik, J. Schaefer, E. O. Stejskal, ACS Symposium Series #40, Molecular Science II, Ed. J. R. Katzer (1977).
4. M. D. Sefcik, H. V. Yuen, Thermochemica Acta 26, 297 (1978).
5. R. M. Barrer, R. M. Gibbons, Trans. Faraday Society, #509 61 (5), 948 (1965).
6. C. T. Ratcliffe, S. N. Vaughn, Div. of Fuel Preprints, Vol. 30, This Symposium.
7. F. J. Long and K. W. Sykes, J. Chem, Phy. 47, 361 (1950).
8. C. A. Mims, J.K. Pabst, Fuel 62(2), 176 (1983).
9. D. W. McKee, Fuel 62(2) 170 (1983).
10. M. J. Vera, A. T. Bell, Fuel, 57, 194 (1978).
11. P. A. Redhead, Vacuum 12, 203 (1962).
12. R. J. Gorte, J. Catalysis, 75 164 (1982).
13. R. J. Cvetanovic and Y. Amenomiya, Adv. in Catalysis, 17, 103 (1967), Catal. Rev. 6 (1), 21-48 (1972).
14. F. S. Feates and C. W. Keep, Trans. Faraday Soc. 66, 3156 (1970).
15. G. Tremblay, F. J. Vastola and P.L. Walker, Jr., Carbon 16, 35 (1978).
16. I. L. C. Freriks, J. M. H. van Wechem, J. C. M. Stuiver, R. Bouwman, Fuel, 60 1463 (1981).
17. J. L. Taylor, W. H. Weinberg, Surf. Sci., 78, 259 (1978).
18. H. Marsh, D. W. Taylor, Fuel, 54, 218 (1975).
19. N. R. Laine, F. J. Vastola, P. L. Walker, Jr., J. Phys. Chem.,67, 2030 (1963).
20. B. J. Wood, R. D. Brittain, K. H. Lau, Division of Fuel Preprints, 28, (1), 55 (1983).
21. J. S. Rieck, A. T. Bell, J. Catalysis 85, 143 (1984).
22. F. Bonner, J. Turkevich, J. Am. Chem. Soc. 73, 561 (1951).
23. F. M. Lang, P. Magnier, Chemistry and Physics of Carbon, Vol. 3, Ed. P. L. Walker, Jr., Marcel Dekker, N. Y., 1968.
24. B. L. Tonge, Proceedings of the Fourth Carbon Conference, 8uffalo, pp. 87-93 (1960).
25. F. J. Long, K. W. Sykes, Proc. Roy. Soc. (London) A215, 100, (1952); J. Gadsby, F. J. Long, P. Sleightholm and K. W. Sykes, Proc. Roy. Soc. (London) A193, 357 (1948).
26. S. Ergun, J. Phys. Chem. 60 480 (1956).
27. S. Ergun, M. Mentser, Chemistry and Physics of Carbon, pp.203, Vol. 1, Ed. P. J. Walker, Jr., Marcel Dekker Inc. 1965.
28. W. T. Tyso, J. Carrazza and G. A. Somorjai, Div. of Fuel Preprints, 29 2, 190 (1984).
29. H. Freund, Fuel, (to be published).

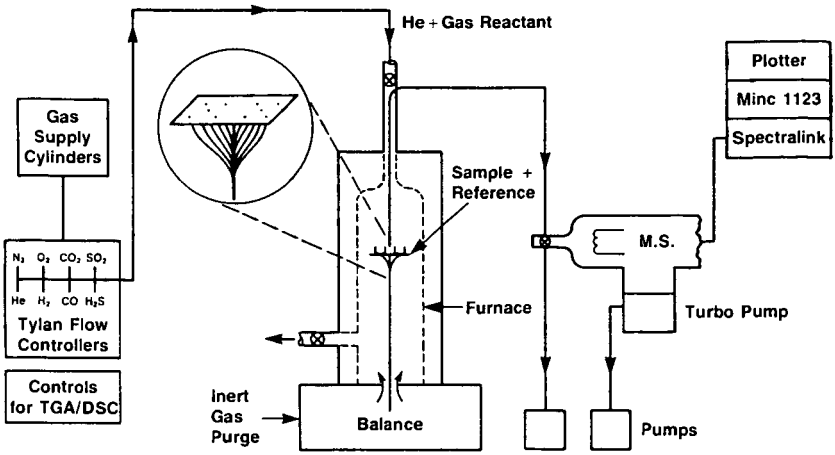

Figure #1. Mettler 2000C Thermal Analysis unit equipped with gas flow control system and on-line M.S. analysis system.

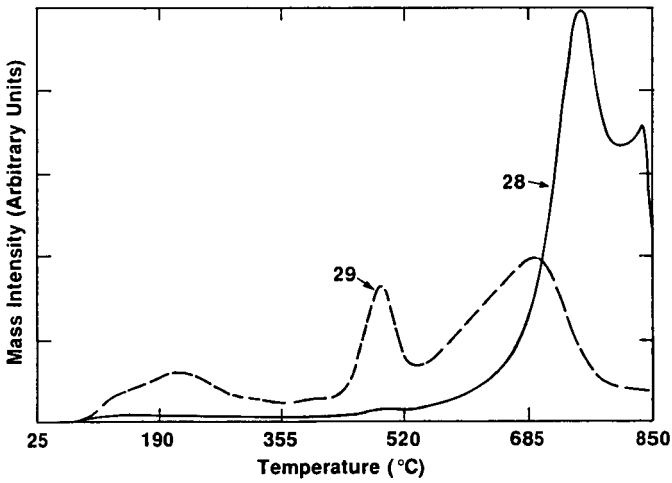

Figure #2. Profile of mass intensity for evolved ^{13}CO (mp=29) and ^{12}CO(m/e=28), temperature programming rate of 0.5 K/s, K-treated Spherocarb powder with $^{13}CO_2$ adsorbed ($\theta \cong 100\%$) at 60°C.

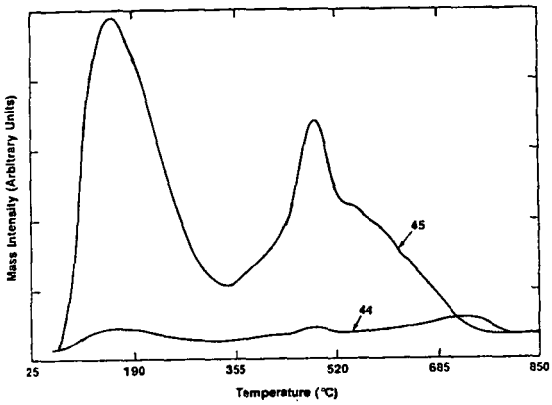

Figure #3. Profile of mass intensities for evolved $^{13}CO_2$(m/e = 45) and $^{12}CO_2$(m/e = 44), Intensity scale magnified 7.5x, same run as Figure #2.

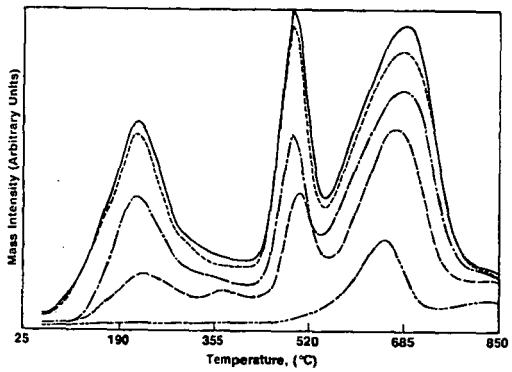

Figure #4. Profile of mass intensity for evolved ^{13}CO (m/e = 29) at different loading levels (θ in %) of $^{13}CO_2$. 1, 6%. 2, 16%. 3, 52%. 4, 76%. 5, 100%.

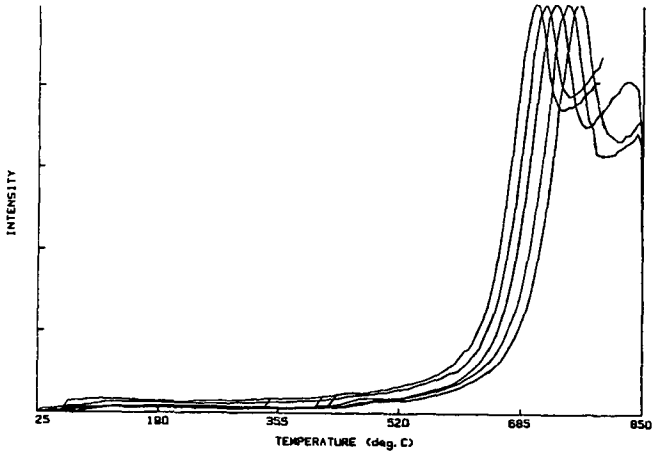

Figure #5. Profile of mass intensities for ^{12}CO desorption (m/e = 28) at different ramping rates (8) 1, 0.083K/sec. 2, 0.125K/sec. 3, 0.167K/sec. 4, 0.0333K/sec. 5, 0.5 K/sec.

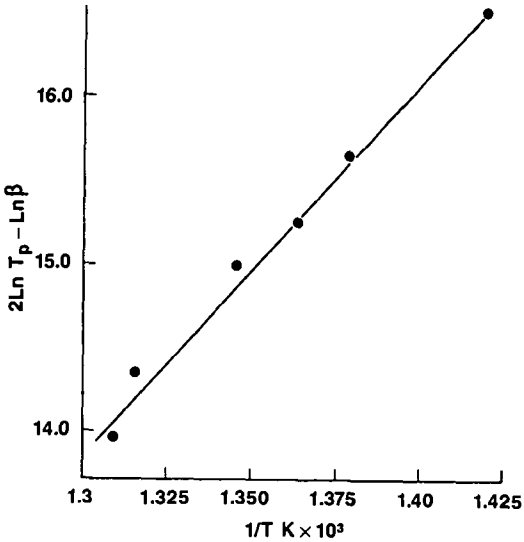

Figure #6. Plot of ^{13}CO desorption values from 420-500°C peak, ΔH from slope 45±3 Kcal/mole, $V_1 = 4x10^{12}$.

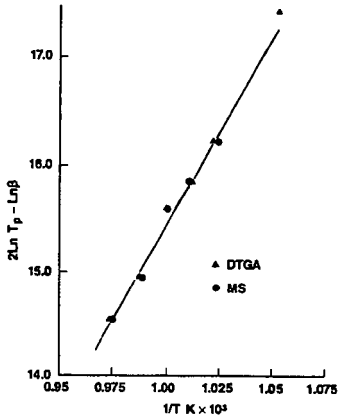

Figure #7. Plot of ^{12}CO desorption values from. 690°C-750°C peak, ΔH from slope 73±3 Kcal/mole, $V_1 = 2x10^{15}$.

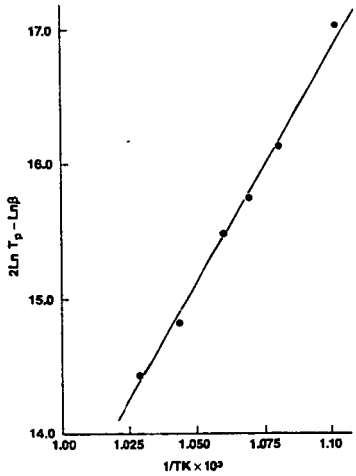

Figure #8. Plot of ^{13}CO desorption values from 650°-690°C peak, ΔH from slope = 72_5 Kcal/mole, $V_1 = 2x10^{16}$.